

Molecular-dynamics study of surface segregation in liquid semiconductor alloys

Wenbin Yu and D. Stroud*

Department of Physics, The Ohio State University, Columbus, Ohio 43210

(Received 16 May 1997)

We report the results of a molecular-dynamics study of the surface tension and surface profile of liquid Si and Ge (ℓ -Si and ℓ -Ge) and their alloys using empirical Stillinger-Weber potentials. The calculations are carried out at two temperatures slightly above the melting temperatures of Si and Ge and the alloys $\text{Si}_{0.8}\text{Ge}_{0.2}$ and $\text{Si}_{0.2}\text{Ge}_{0.8}$. They show clear evidence of surface segregation by Ge, the component with the lower surface tension. [S0163-1829(97)05843-8]

I. INTRODUCTION

It is widely believed that the surface tension of liquids is strongly affected by impurities. An impurity with a lower surface tension than that of the host will have a tendency to migrate towards the surface, thereby lowering the surface tension and hence the free energy of the mixture. Conversely, a high-surface-tension impurity is expected to migrate *away* from the surface, again so as to lower the free energy of the mixture. If the difference in surface tensions is sufficiently large, or if the two components have only a slightly negative free energy of mixing, this tendency may actually be sufficient to cause the two components to phase separate — for example, a low-surface-tension impurity may exist mostly as a surface layer. Even when the difference in surface tensions is not large, this effect may still be sufficient to cause an excess of low-surface-tension impurity, or a deficit of one with high-surface tension, near the liquid surface.

Convincing evidence of such surface segregation is time consuming to obtain in numerical simulations. In order to use standard methods, such as Monte Carlo or molecular-dynamics simulations, one must deal with free surfaces (usually *two* free surfaces). Because of this inhomogeneity, it is necessary to treat relatively large systems in order to obtain numerically convincing results. In addition, one must use various tricks to make sure that the system ends up in an equilibrium configuration, and that the various quantities of interest (such as density profiles and surface tensions) are calculated as suitable equilibrium averages.

In this paper, we carry out a simulation of a much studied liquid alloy, $\text{Si}_x\text{Ge}_{1-x}$, using standard empirical potentials and a simulation system of 8000 atoms, in combination with molecular-dynamics techniques. We have chosen this system for several reasons. First, both its bulk and its surface properties are of considerable experimental interest, especially because of the role of these materials in processing the corresponding solid semiconductors.¹⁻⁷ Second, numerous calculations have been carried out in both the liquid elements and the alloys.⁸⁻²³ These calculations use a variety of mostly numerical techniques (such as Monte Carlo and molecular dynamics) in combination with both empirical potentials and *ab initio* interactions derived from density-functional theories of electronic structure. Finally, an earlier calculation,¹¹ using empirical potentials and Monte Carlo algorithm, gave a hint of such surface segregation in a small-scale simulation

of 216 atoms. Our calculations, also based on empirical potentials, provide strong evidence for such surface segregation based on simulations of 8000 atoms.

We treat the liquid alloy using a set of empirical two-body and three-body interactions of the form originally proposed by Stillinger and Weber (SW).⁹ These interactions have the convenience of being independent of density. They also give a reasonable approximation to the structure factors in the liquid state, which have unusual shoulders on the principal peak thought to arise from bond-angle-dependent interatomic forces. While they do not give good accounts of many properties, such as electrical conductivity, which obviously depend on electronic degrees of freedom, they can be used to treat large disordered systems. In the present work, we treat a sample of 8000 atoms with two free surfaces; if it were necessary, much larger systems could actually be treated using the same method.²⁴ To calculate the surface properties, we use a standard molecular-dynamics (MD) approach in the presence of a free surface. The surface tension itself is computed as an integral over appropriate elements of the surface stress tensor, while the partial density profiles near the surface are calculated as MD averages.

We now turn to the body of the paper. The next section summarizes both our model and the numerical techniques used to implement it; a more detailed description can be found elsewhere.²² The following section presents our results, which are then discussed briefly in the concluding section.

II. MODEL AND METHOD OF CALCULATION

A. Empirical potential for interatomic interactions

We treat the Si-Si, Si-Ge, and Ge-Ge interactions as a sum of two-body and three-body interactions of the form introduced by Stillinger and Weber.⁹ These interactions may be written in the form

$$\Phi = \sum_{i < j} \epsilon f_2(r_{ij}/\sigma) + \sum_{i < j < k} \lambda \epsilon f_3(\vec{r}_i/\sigma, \vec{r}_j/\sigma, \vec{r}_k/\sigma), \quad (1)$$

where $f_2(x)$ and $f_3(\vec{x}_1, \vec{x}_2, \vec{x}_3)$ take the form given in Ref. 9. The form of Φ depends on the parameters ϵ (which governs the strength of the two-body potential), σ (which describes the range of that potential), and λ (which measures the relative strength of the three-body and two-body potentials). In

TABLE I. Stillinger-Weber parameters for Si-Si and Ge-Ge interactions. The Si-Ge parameters are obtained from these as described in the text.

| | ϵ (eV) | σ (Å) | λ |
|----|-----------------|--------------|-----------|
| Si | 2.315 | 2.0951 | 21 |
| Ge | 1.74 | 2.215 | 19.5 |

the present calculations, we use values for these parameters taken from our previous work on the self-diffusion coefficients of liquid Si and Ge.²² These values are shown in Table I. For the Si-Ge potential, we use the geometric mean of the Si-Si and Ge-Ge values for ϵ and λ , and the arithmetic mean for σ , as described in our previous paper.²²

It may be useful to comment on the reasons for our choice of the parameters ϵ , λ , and σ in the Si-Ge potential, since this choice has a strong influence on the degree of surface segregation in the liquid. First, this choice has been made by several other groups in studies of *solid* surfaces of SiGe alloys.^{25–29} Similarly, in simulations of mixtures using Lennard-Jones potentials, there is a time-honored tradition of choosing the geometric mean for the strength parameter ϵ and the arithmetic mean for the range parameter σ ,³⁰ in analogy with our choice here.

On a more basic level, our choice is reasonable, though difficult to derive from first principles. If we take the (over-simplified) view that σ is an effective hard-sphere diameter, then the effective σ between unlike atoms would indeed be the arithmetic mean of those between like atoms, as assumed here. As for the choice of geometric averaging for the strength parameters ϵ and λ , we note only that such a choice is rigorously justifiable for the $1/r^6$ part of a Lennard-Jones potential: in that case, the strength of the attractive tail is proportional to the products of the polarizabilities of the two interacting atoms.

Clearly, it would be useful to have some explicit way of testing the validity of this approximation. An ideal test would probably involve a comparison of the three partial structure factors, as calculated from our potentials, to experiment. Such a calculation could readily be done, but at present, no experimental data appears to be available for comparison. We note also another, though not very demanding, requirement satisfied by the potentials: the bulk liquid alloy described by these potentials is stable against phase separation, in agreement with experiment.

B. Computational procedure and geometry of simulation cell

Our calculations make use of a standard MD procedure. We use an 0.5 fs MD time step to integrate Newton's equations of motion, using the standard velocity-Verlet algorithm.³⁰ All the simulations are initialized in a bulk crystalline state in the diamond structure, containing 8000 atoms and with periodic boundary conditions (PBC's). These simulations begin at 2500 K for Si and 2100 K for Ge, and the system is then gradually cooled (at a rate of 100 K/3 ps) to final values of about 1700 and 1900 K for ℓ -Si and about 1300 and 1500 K for ℓ -Ge. As the system is being cooled, we continuously perform MD simulations in the (N, P, T)

TABLE II. Results of simulations for bulk ℓ -Si and ℓ -Ge. T denotes the average temperature in K; L is the edge of the simulation cell, in Å; ρ is the density; $\langle P \rangle$ is the average pressure; and $\langle E_v \rangle$ is the average internal potential energy. $\langle \rangle$ denotes an ensemble average.

| Property | Liquid Si | | Liquid Ge | |
|--|------------|------------|------------|------------|
| | $T=1700$ K | $T=1900$ K | $T=1300$ K | $T=1500$ K |
| L (Å) | 53.364 | 53.437 | 55.732 | 55.897 |
| ρ (g/cm ³) | 2.455 | 2.445 | 5.778 | 5.521 |
| $\langle P \rangle$ (10 ⁻² GPa) | -3.08 | 1.19 | 2.04 | 2.45 |
| $\langle E_v \rangle$ (eV) | -4.0504 | -4.0051 | -3.1195 | -3.0851 |

ensemble in order to maintain zero internal pressure P at all temperatures. [This ensemble is appropriate in the presence of periodic boundary conditions, because it corresponds to the actual state of the bulk system (with $P = 0$).] At the end of this cooling, an additional 15 ps of (N, P, T) simulations are carried out at $P=0$, and the average size of the simulation box is obtained over the last 10 ps of these simulations.

Once these calculations are completed, we switch to MD simulations in the (N, V, T) ensemble, using velocity-rescaling method to equilibrate the kinetic energy to the desired temperatures. An (N, V, T) ensemble is appropriate

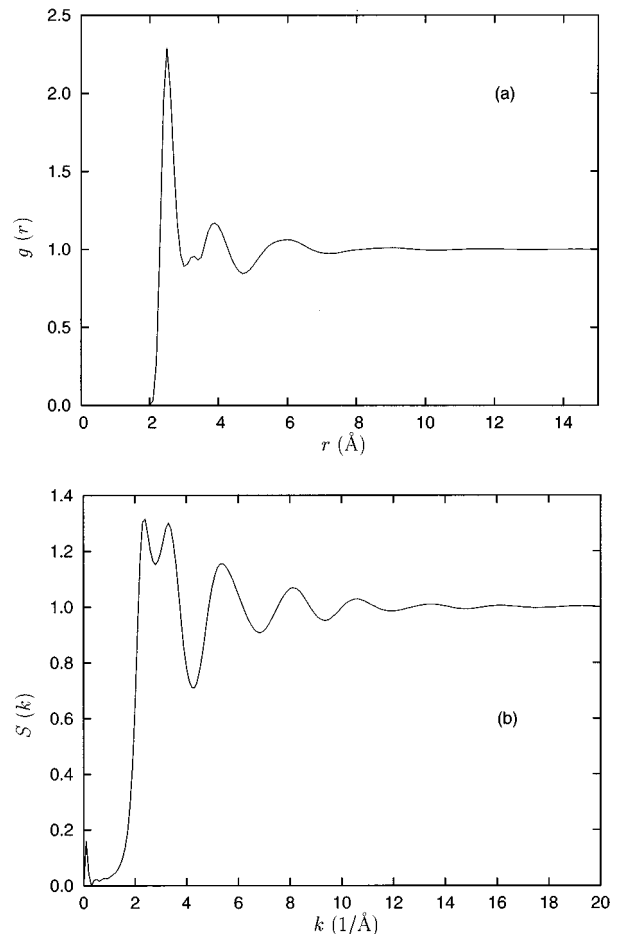


FIG. 1. (a) and (b) Pair distribution function $g(r)$ and structure factor $S(k)$ for ℓ -Si at 1700 K, as obtained by MD simulation.

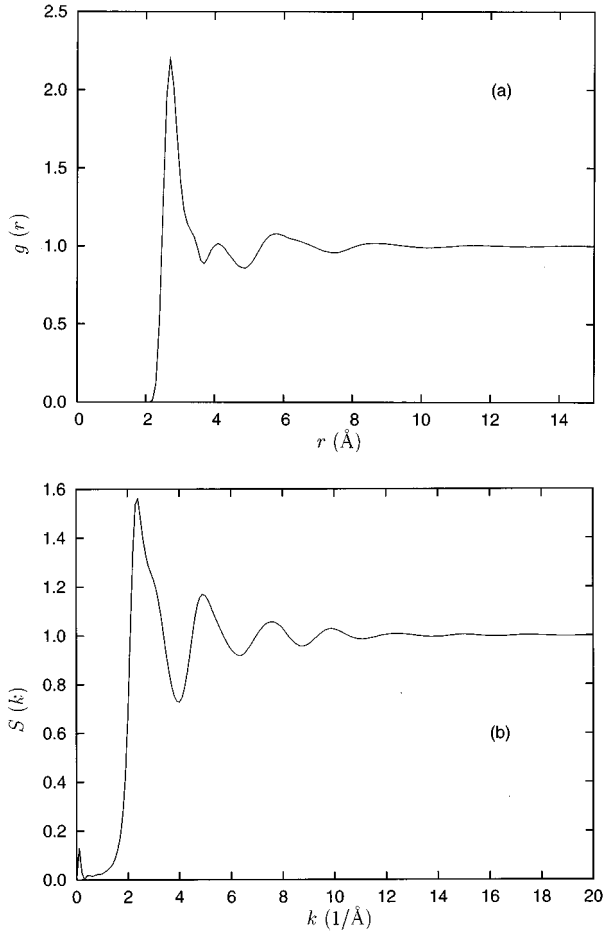


FIG. 2. Same as Fig. 1, but for ℓ -Ge at 1300 K.

here, because a simulation at fixed pressure is not feasible with free surfaces — the liquid would undergo an unphysical expansion in the direction of the free surfaces. These simulations are carried on for 5 ps, using the previously obtained average simulation cell size V .

Finally, we switch to MD simulations in the (N, V, E) ensemble for 15 ps. This last switch is done purely for calculational convenience: once thermalization has been

achieved, it is easier to collect MD simulation results in the (N, V, E) rather than (N, V, T) ensemble, since the equations of motion are then fully deterministic. Our simulations show, however, that the temperature fluctuates very little in the (N, V, E) ensemble — by less than 10 K — implying that we would have attained similar results even if we had continued to work in the (N, V, T) ensemble in the last part of the simulation. Results from the last 10 ps of these (N, V, E) simulations are used to obtain the average internal potential energy $\langle E_v \rangle$, and the average internal pressure $\langle P \rangle$.

We use the configuration obtained from the bulk (N, V, E) simulations after 5 ps as the starting point for the pure liquid slab simulations. Thus, after 5 ps, we remove the periodic boundary conditions from the two opposite faces of the simulation box in the z direction, so that the system has two free surfaces facing the $\pm z$ directions. We then run MD in the (N, V, T) ensemble (again using the velocity-rescaling algorithm) for 5 ps to equilibrate the slab system to the temperature of the corresponding bulk liquid. Then we switch to MD simulations in the (N, V, E) ensemble for 25 ps, using the final 20 ps to calculate various averaged properties, including the internal potential energy, the surface stress tensor, and the surface tension.

After completing the slab (N, V, T) MD simulations just described, in addition to carrying out (N, V, E) MD for the pure liquid slab systems, we also begin new simulations for liquid slabs containing impurities. In the liquid Si slab, we replace 20% of the Si atoms (i.e., 1600 atoms) by Ge atoms; and in the liquid Ge slab, we replace 20% of the Ge atoms by Si atoms. Following these replacements, we first run 5 ps of MD simulations in the (N, V, T) ensemble (with velocity rescaling) to equilibrate the system to the temperatures of the corresponding pure slab systems. Then we switch to (N, V, E) MD simulations, in order to study various phenomena arising from impurity segregation.

A natural concern in these seemingly high-temperature calculations is that some of the atoms might start to evaporate from the free surfaces. However, in all of our slab simulations, not a single atom was ever observed to evaporate from any free surfaces, even though some of the simulations were run for as long as 0.2 ns. Another possible concern is that the slab might bend during the simulations, since there is

TABLE III. Results of simulations for slabs of pure ℓ -Si and pure ℓ -Ge. T is the average temperature; L is the simulation cell edge in the horizontal direction (i.e., L^2 is the area of the free surface); $\langle E_v \rangle$ is the average internal potential energy; $\langle E_s \rangle$ is the average surface energy; σ_{xx} , σ_{yy} , and σ_{zz} are components of the surface stress tensor; and γ is the surface tension. The quoted error is an estimate of the statistical uncertainty involved in calculating γ , as obtained using the procedure of Ref. 30.

| Property | Liquid Si | | Liquid Ge | |
|---|-------------|-------------|-------------|-------------|
| | $T=1700$ K | $T=1900$ K | $T=1300$ K | $T=1500$ K |
| L (Å) | 53.364 | 53.437 | 55.732 | 55.897 |
| $\langle E_v \rangle$ (eV) | -4.0068 | -3.9649 | -3.0846 | -3.0522 |
| $\langle E_s \rangle$ (eV/Å ²) | 0.1225 | 0.1127 | 0.0899 | 0.0843 |
| $\langle \sigma_{xx} \rangle$ (10 ⁻² eV/Å ²) | 3.04 | 2.89 | 2.34 | 2.52 |
| $\langle \sigma_{yy} \rangle$ (10 ⁻² eV/Å ²) | 2.86 | 2.82 | 2.20 | 2.44 |
| $\langle \sigma_{zz} \rangle$ (10 ⁻² eV/Å ²) | 0.08 | 0.01 | -0.02 | 0.19 |
| $\langle \gamma \rangle$ (10 ⁻² eV/Å ²) | 2.87 ± 0.11 | 2.85 ± 0.17 | 2.29 ± 0.08 | 2.29 ± 0.09 |

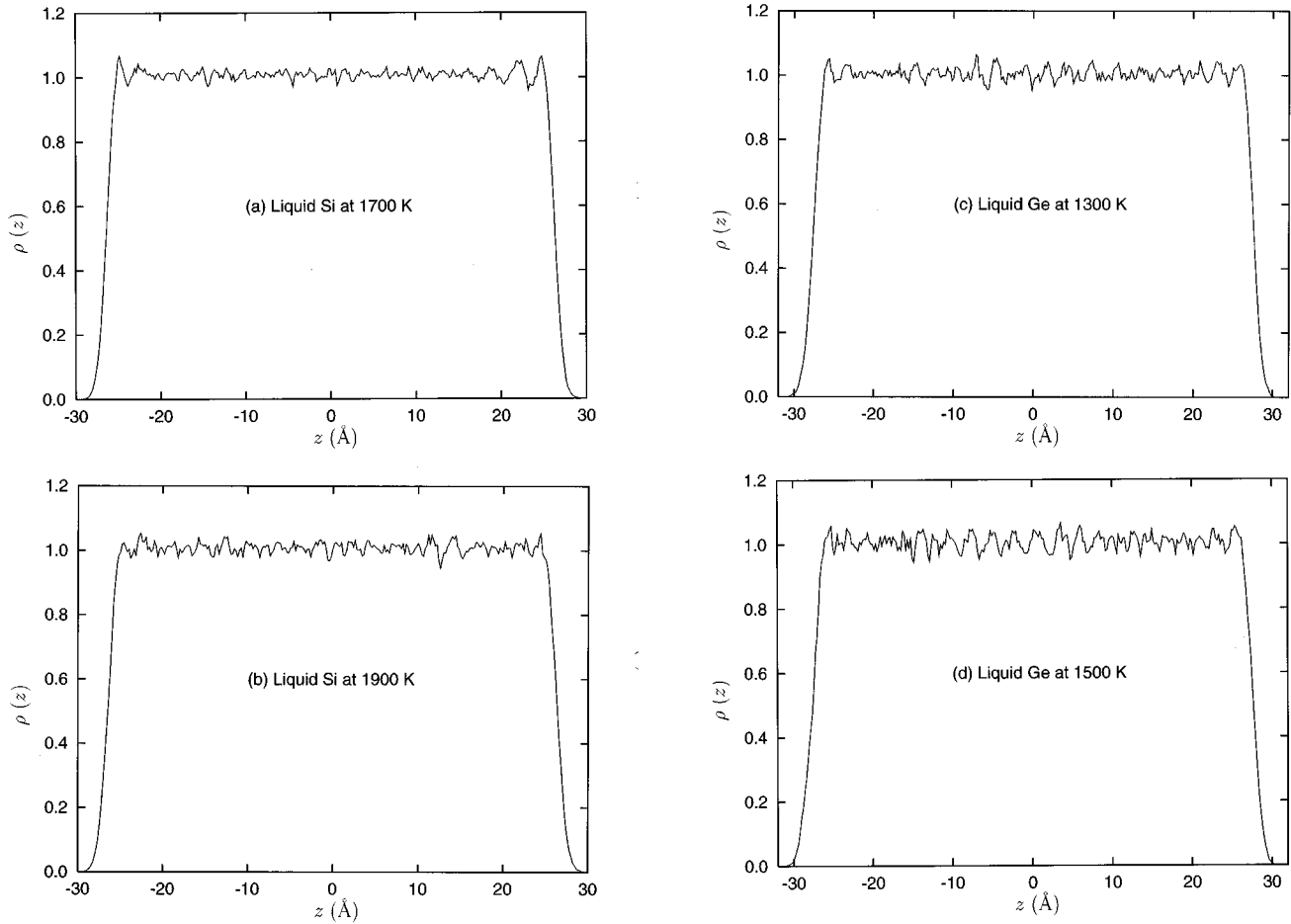


FIG. 3. Density profiles $\rho(z)$ for slabs of pure liquid semiconductors with two free surfaces, calculated by MD simulations as described in the text. The densities are normalized to the atom number densities of pure bulk ℓ -Si and ℓ -Ge at the temperatures shown. (a) and (b) ℓ -Si at 1700 K and 1900 K. (c) and (d) ℓ -Ge at 1300 K and 1500 K.

no constraint preventing such bending. But for the sample sizes considered (of linear dimensions about 55 Å), no such bending was ever observed, presumably because of the very large energy required to produce bending in a sample of such small area.

C. Calculation of surface stress and surface tension

The surface tension γ of the liquid is most easily calculated directly from the interatomic interactions, i.e., using the mechanical expressions for the surface stress.^{31,32} Thus γ is computed from

$$\gamma = \frac{1}{2}(\sigma_{xx} + \sigma_{yy} - 2\sigma_{zz}). \quad (2)$$

Here the $\sigma_{\alpha\beta}$'s are components of the surface stress tensor, defined by³³

$$\sigma_{\alpha\beta} = -\frac{1}{S} \sum_i \left[\frac{p_i^\alpha p_i^\beta}{m_i} + \frac{1}{4} \sum_j (r_{ij}^\beta f_{ij}^\alpha + r_{ij}^\alpha f_{ij}^\beta) \right], \quad (3)$$

where $(\alpha, \beta) \equiv (x, y, z)$, S is the surface area, m_i and \vec{p}_i are the mass and momentum of atom i , \vec{r}_{ij} is the distance from atom i to j , \vec{f}_{ij} is the force on atom i due to atom j , and both the summations over i and j run over all the atoms in the

systems. Although the summation runs over all the atoms in the volume, the primary contribution comes from atoms near the surface, so that this expression remains finite even if the sample is very thick.

III. RESULTS

Our results for pure bulk liquid Si and Ge, all carried out with 8000 atoms, are shown in Table II, and in Figs. 1 and 2. The empirical potentials predict a small positive coefficient of thermal expansion for ℓ -Ge and virtually no thermal expansion for ℓ -Si, possibly because of small deviations in the calculated pressure from zero. The principal peak in the structure factor of ℓ -Ge shows a shoulder on the high- q side, in agreement with experiment.

In the temperature range we have explored for ℓ -Si and ℓ -Ge, roughly from the melting temperatures to about 1000 K higher, the position of this shoulder is nearly independent of temperature though the shoulder gets weaker as the temperature is increased (this behavior is not shown in the figure, however). The strength of the shoulder is quite sensitive to the choice of parameters of σ and λ . For the present choice of parameters, the SW potential predicts a shoulder in Si which is too strong, in comparison with experiments^{3,4} (in the experiments, this peak is a shoulder rather than the sec-

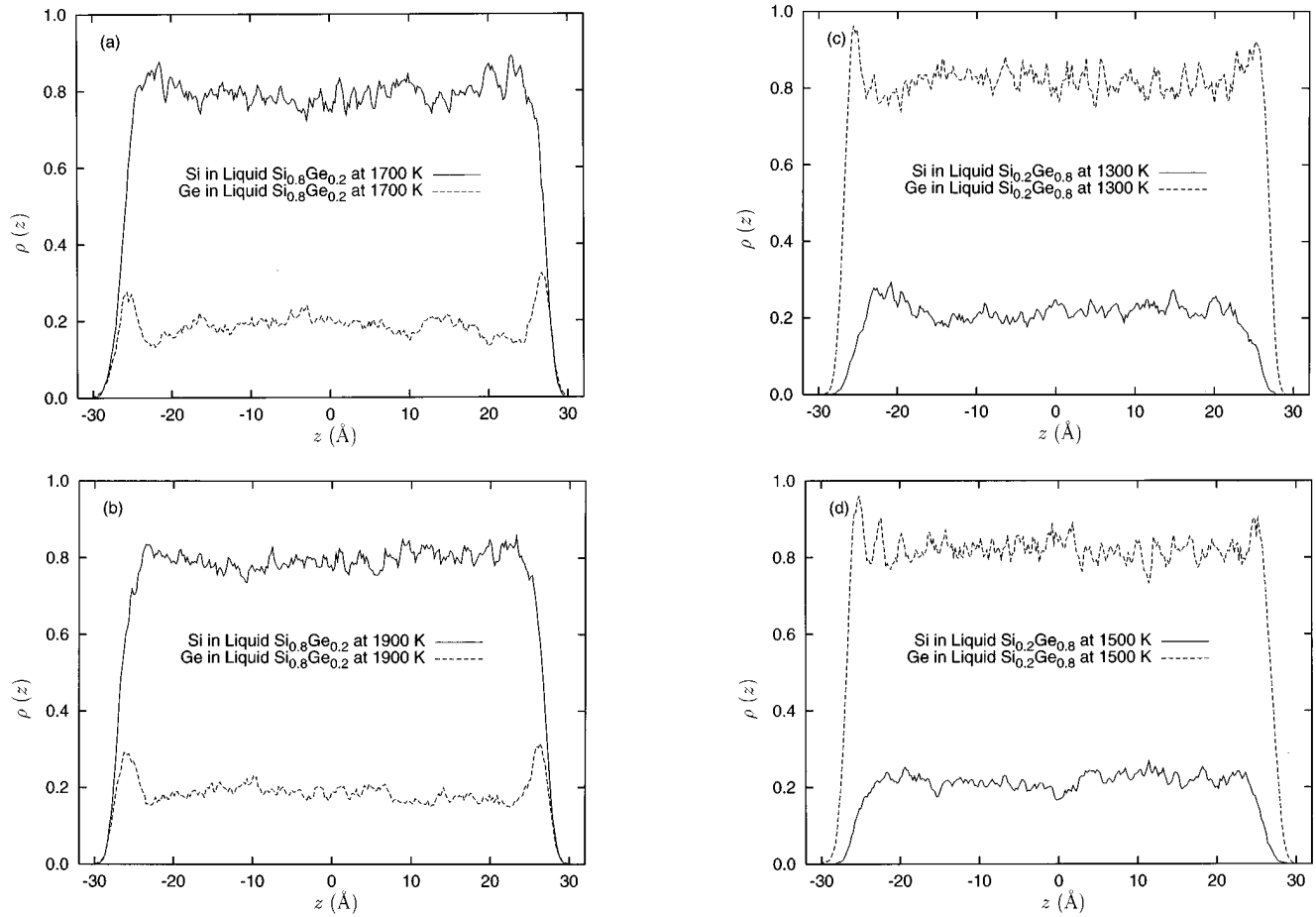


FIG. 4. Density profiles $\rho_{\text{Si}}(z)$ and $\rho_{\text{Ge}}(z)$ for two concentrations and two temperatures as indicated in the legends. The densities are normalized to the atom number densities of pure host bulk ℓ -Si and ℓ -Ge at the temperatures shown.

ondary peak as here); agreement between theory and experiment for Ge is good. A similar quality of agreement has been shown in our previous paper²² using the SW potential with the same parameters, and in the work of many other groups.^{9,10,21}

The structure factors of ℓ -Si and ℓ -Ge have also been calculated by many *ab initio* simulations^{8,14,18,19,23} and the results generally agree very well with experimental measurements. The agreement is, in fact, probably superior to that obtained with empirical potentials — in particular, the shoulder in the structure factor has a strength which matches experiment very well. As there is no arbitrarily adjustable parameters in these calculations, and as they properly include the electronic as well as ionic degrees of freedom, these simulation results are likely to be more reliable than in the empirical case, though such calculations also suffer from being applicable only to small systems (several hundreds of particles).

Table III shows the corresponding results for pure ℓ -Si and ℓ -Ge with free surfaces. Of greatest interest here are the calculated surface tensions. These do not change substantially with temperature to within the statistical accuracy of our calculations. The calculated Si surface tension value agrees with the experimental value of $5.53 \text{ eV}/\text{\AA}^2$ (Ref. 6) within a factor of two. The density profiles (shown in Fig. 3) show that the free surface density profiles of both ℓ -Si and

ℓ -Ge are monotonic. We believe that the small oscillations seen within the interiors of the slabs at all temperatures are simply the consequences of not having run large enough systems for long enough times. As evidence for this conclusion, we note that earlier simulations run on the same model but with only 216 atoms¹¹ show much larger oscillations.

The most striking results of our simulations are shown in Fig. 4, which shows the partial density profiles of Si and Ge at two different concentrations and two different temperatures. Each profile is the result of an average over 10 ps following equilibration of the slab. In this figure, we see clear evidence of the surface segregation which was only hinted at in previous simulations using the same model.¹¹ In both alloys, the component with the smaller surface tension, namely, Ge, is driven towards the surface. This behavior can be understood, we believe, by considering two related effects: (i) the Ge atoms are slightly larger than the Si atoms; and (ii) [partly as a consequence of (i)] ℓ -Ge has weaker interatomic interactions than ℓ -Si as shown in Table II. Because the atomic size difference is quite small and the interatomic interactions are similar, Si and Ge are mutually soluble at all concentrations in the liquid (and also in the solid) for temperatures above room temperature. Nevertheless, the differences in atom size and interatomic interactions cause the Ge to have a somewhat lower surface tension than

TABLE IV. Results of simulations for slabs of liquid $\text{Si}_x\text{Ge}_{1-x}$ alloys. Symbols are the same as in Table III.

| Property | Liquid $\text{Si}_{0.8}\text{Ge}_{0.2}$ | | Liquid $\text{Si}_{0.2}\text{Ge}_{0.8}$ | |
|---|---|------------|---|------------|
| | $T=1700$ K | $T=1900$ K | $T=1300$ K | $T=1500$ K |
| $\langle\sigma_{xx}\rangle$ (10^{-2} eV/Å ²) | 2.62 | 2.61 | 2.38 | 2.31 |
| $\langle\sigma_{yy}\rangle$ (10^{-2} eV/Å ²) | 2.65 | 2.60 | 2.33 | 2.29 |
| $\langle\sigma_{zz}\rangle$ (10^{-2} eV/Å ²) | -0.02 | -0.02 | 0.00 | 0.04 |
| $\langle\gamma\rangle$ (10^{-2} eV/Å ²) | 2.65 | 2.63 | 2.36 | 2.26 |

the Si. This difference provides, at all alloy concentrations, a driving force which tends to push the Ge atoms towards the free surface.

The tendency toward surface segregation is most conspicuous in the $\text{Si}_{0.8}\text{Ge}_{0.2}$ alloys, where we see a clear peak in Ge concentration near the free surfaces. We find that the average concentration of Ge in the surface layer (defined as the layer starting from the first minimum on the interior side of the Ge surface peak) is about 0.25 at 1700 K and 0.26 at 1900 K; both values are clearly higher than the overall average value of 0.20. In the $\text{Si}_{0.2}\text{Ge}_{0.8}$ alloy, the clearest effect is that the Si atoms are pushed *away* from the surface, leaving a layer of Si-poor alloy near the surface. There is still a peak in Ge concentration near the surface, but it is weaker than in at the other concentration (as it must be, in order to conserve quantities of each atomic species in both cases). The average Si concentration in the surface layer is approximately 0.13 at 1300 K and 0.14 at 1500 K, both of which are clearly *lower* than the overall average value of 0.20.

Although our simulations are directed at equilibrium rather than dynamical properties, we can still make some approximate statements about the rate of segregation. For example, the surface profiles shown become time independent after, at most, 20 – 30 ps of simulation. If we assume that this profile is formed by excess Ge atoms diffusing from the interior of the slab to the surface, then an *order-of-magnitude* estimate of the corresponding diffusion constant would be $D_{\text{SiGe}} \approx r^2/(6t)$, where r is the distance diffused and $t \approx 20$ ps. If we take $r \approx 5$ Å, this estimate gives $D_{\text{SiGe}} \approx 0.2 \times 10^{-4}$ cm²/sec, slightly smaller than the diffusion coefficient estimated for pure liquid Si or Ge using Stillinger-Weber potentials.¹¹ This value should not be taken very seriously, however, since it is based only on a rough estimate of equilibration time for our surface profile.

Another consequence of the surface segregation can be seen in the tabulated surface tensions (see Table IV). Namely, the surface tensions of both alloys lie below a straight line (i.e., linear in concentration) interpolation of the elemental surface tensions. While this effect is not large (of order 10^{-3} eV/Å), it is clearly real and not just an artifact of statistical fluctuations. The explanation is straightforward: the component with the lower surface tension migrates toward the surface, thereby giving not only an excess surface concentration of that component but also a surface tension which lies below a linear interpolation of the pure components.

IV. DISCUSSION

The surface segregation we calculate here is not surprising: free energy minimization should drive the component with the lower surface tension towards the liquid surface, and our simulations confirm this. Nonetheless, it is impressive how extensively this segregation occurs, since the two components (Si and Ge) have very similar properties as pure liquids, quite similar densities, and not very different surface tensions. To our knowledge, no experiment has been carried out which directly confirms this segregation; clearly a measurement sensitive to one of the two atomic species would be most useful here.

Although it would be ideal to avoid the use of empirical potentials in these calculations, this would not be easy in an MD calculation. An *ab initio* approach, such as has been used to calculate some bulk properties of liquid metals, is typically limited to several hundreds of atoms. With this number of atoms, one could not obtain reliable information about surface segregation. Various approximate theories of surface tension and profiles in liquid alloys might be useful, but these would have different kinds of uncertainties. Because of our use of empirical potentials, however, we do not believe that the numerical values of our surface tensions are likely to be accurate. Nevertheless, the surface segregation seen in our calculations should occur no matter what specific potentials are used in the simulations.

To conclude, we have carried out MD simulations of liquid $\text{Si}_x\text{Ge}_{1-x}$ alloys in the presence of a free surface, using empirical two- and three-body interatomic interactions. We find that Ge (the low surface tension component) tends to surface segregate at both low and high alloy concentrations of Ge. This behavior is not likely to be unique to this material, but should occur widely in liquid alloy systems. It would be of considerable interest if this surface segregation could be detected experimentally.

ACKNOWLEDGMENTS

We gratefully acknowledge useful conversations with D. Matthiesen, A. Chait, A. Velosa, Z. Q. Wang, and R. V. Kulkarni. This work has been supported by the Microgravity Sciences Division of the National Aeronautics and Space Administration, through Grant No. NAG3-1437.

*Electronic address: stroud@ohstpy.mps.ohio-state.edu

- ¹P. V. Pavlov and E. V. Dobrokhotov, *Fiz. Tverd. Tela (Leningrad)* **12**, 281 (1970) [*Sov. Phys. Solid State* **12**, 225 (1970)].
- ²K. M. Shvarev, B. A. Baum, and P. V. Gel'd, *Fiz. Tverd. Tela (Leningrad)* **16**, 3246 (1974) [*Sov. Phys. Solid State* **16**, 2111 (1975)].
- ³Y. Waseda and K. Suzuki, *Z. Phys. B* **20**, 339 (1975).
- ⁴J. P. Gabathuler and S. Steeb, *Z. Naturforsch. A* **34**, 1314 (1979).
- ⁵C. F. Hague, C. Sénémaud, and H. Ostrowiecki, *J. Phys. F* **10**, L267 (1980).
- ⁶S. Hardy, *J. Cryst. Growth* **69**, 456 (1984).
- ⁷H. Sasaki, E. Tokizaki, K. Terashima, and S. Kimura, *J. Cryst. Growth* **139**, 225 (1994).
- ⁸R. Car and M. Parrinello, *Phys. Rev. Lett.* **55**, 2471 (1985).
- ⁹F. H. Stillinger and T. A. Weber, *Phys. Rev. B* **31**, 5262 (1985).
- ¹⁰J. Q. Broughton and X. P. Li, *Phys. Rev. B* **35**, 9120 (1987).
- ¹¹Z. Q. Wang and D. Stroud, *Phys. Rev. B* **38**, 1384 (1988).
- ¹²A. Arnold, N. Mauser, and J. Hafner, *J. Phys.: Condens. Matter* **1**, 965 (1989).
- ¹³W. Jank and J. Hafner, *Phys. Rev. B* **41**, 1497 (1990).
- ¹⁴I. Štich, R. Car, and M. Parrinello, *Phys. Rev. Lett.* **63**, 2240 (1989); *Phys. Rev. B* **44**, 4262 (1991).
- ¹⁵R. Virkkunen, K. Laasonen, and R. M. Nieminen, *J. Phys.: Condens. Matter* **3**, 7455 (1991).
- ¹⁶C. Z. Wang, C. T. Chan, and K. M. Ho, *Phys. Rev. B* **45**, 12227 (1992).
- ¹⁷J. R. Chelikowsky, N. Troullier, and N. Binggeli, *Phys. Rev. B* **49**, 114 (1994).
- ¹⁸G. Kresse and J. Hafner, *Phys. Rev. B* **49**, 14251 (1994).
- ¹⁹N. Takeuchi and I. L. Garzón, *Phys. Rev. B* **50**, 8342 (1994).
- ²⁰K. Kakimoto, *J. Appl. Phys.* **77**, 4122 (1995).
- ²¹M. Ishimaru, K. Yoshida, and T. Motooka, *Phys. Rev. B* **53**, 7176 (1996).
- ²²W. Yu, Z. Q. Wang, and D. Stroud, *Phys. Rev. B* **54**, 13946 (1996).
- ²³R. Kulkarni, W. G. Aulbur, and D. Stroud, *Phys. Rev. B* **55**, 6896 (1997).
- ²⁴W. Yu and A. Madhukar, *Phys. Rev. Lett.* **79**, 905 (1997).
- ²⁵M. H. Grabow and G. H. Gilmer, *Surf. Sci.* **194**, 333 (1988).
- ²⁶P. C. Weakliem and E. A. Carter, *Phys. Rev. B* **45**, 13458 (1992).
- ²⁷M. Karimi, T. Kaplan, M. Mostoller, and D. E. Jesson, *Phys. Rev. B* **47**, 9931 (1993).
- ²⁸C. Roland and G. H. Gilmer, *Phys. Rev. B* **47**, 16286 (1993).
- ²⁹L. E. Carter, P. C. Weakliem, and E. A. Carter, *J. Vac. Sci. Technol. A* **11**, 2059 (1993).
- ³⁰M. P. Allen and D. J. Tildesley, *Computer Simulation of Liquids* (Clarendon Press, Oxford, 1987).
- ³¹J. K. Lee, J. A. Barker, and G. M. Pound, *J. Chem. Phys.* **60**, 1976 (1974).
- ³²J. Miyazaki, J. A. Barker, and G. M. Pound, *J. Chem. Phys.* **64**, 3364 (1976).
- ³³V. Vitek and T. Egami, *Phys. Status Solidi B* **144**, 145 (1987).